

# Compositional evolution of SiGe islands on patterned Si (001) substrates

Jianjun Zhang<sup>1</sup>, Armando Rastelli, Oliver G. Schmidt, and Günther Bauer

Citation: *Appl. Phys. Lett.* **97**, 203103 (2010); doi: 10.1063/1.3514239

View online: <http://dx.doi.org/10.1063/1.3514239>

View Table of Contents: <http://aip.scitation.org/toc/apl/97/20>

Published by the [American Institute of Physics](#)

---

---

**Fearful for the future of science?**

Sign up for **FREE** FYI emails.  
AIP | American Institute of Physics

# Compositional evolution of SiGe islands on patterned Si (001) substrates

Jianjun Zhang,<sup>1,2,a)</sup> Armando Rastelli,<sup>2</sup> Oliver G. Schmidt,<sup>2</sup> and Günther Bauer<sup>1</sup>

<sup>1</sup>Institute of Semiconductor and Solid State Physics, University Linz, A-4040 Linz, Austria

<sup>2</sup>Institute for Integrative Nanosciences, IFW Dresden, Helmholtzstr. 20, D-01069 Dresden, Germany

(Received 17 September 2010; accepted 19 October 2010; published online 15 November 2010)

The authors investigate, by atomic-force-microscopy-based nanotomography, the composition evolution of ordered SiGe islands grown on pit-patterned Si (001) substrates as their size and aspect ratio increase with increasing Ge deposition. Compared to islands grown on flat substrates, the ordered island arrays show improved size, shape, and compositional homogeneity. The three-dimensional composition profiles of individual pyramids, domes, and barns reveal that the Ge fraction at the base and in subsurface regions of the islands decreases with increasing amount of deposited Ge. © 2010 American Institute of Physics. [doi:10.1063/1.3514239]

The alloy distribution in strained epitaxial islands obtained in the Stranski–Krastanow growth mode is crucial in determining their optical and electronic properties. When the growth is performed on planar substrates, the island ensembles are characterized by rather broad size and shape distributions because of the stochastic processes responsible for their growth.<sup>1–4</sup> Island coarsening, consisting in the growth of larger islands at the expense of smaller ones through material exchange, also contributes to the broadening of the distributions.<sup>5,6</sup> In contrast, when growth is performed on regularly spaced pit-patterned substrates, the driving force for coarsening is effectively reduced.<sup>7–11</sup> Each pit can be in fact considered as the center of a capture zone and represents a local minimum of the chemical potential. Our recent studies have focused on the morphological evolution of SiGe island arrays on pit-patterned substrates.<sup>8</sup>

In this letter, we focus on the compositional evolution of ordered SiGe islands, which we study by a nanotomography technique relying on selective wet chemical etching and atomic force microscopy (AFM).<sup>10,12</sup> We find that the island arrays on patterned substrates are not only morphologically but also compositionally homogeneous and each island shows a symmetric alloy distribution. In contrast, for islands on planar substrates, slight lateral asymmetries in the composition are generally observed, even for islands with an apparently symmetric shape. With increasing Ge deposition, all islands on patterned substrates evolve simultaneously in size, shape, and composition. Finally, the detailed analysis of the composition profiles of islands at different stages of their evolution (pyramids, domes, and barns)<sup>8,13</sup> reveals that the Ge fraction at the base and in subsurface regions of the islands slightly decreases with increasing amount of deposited Ge.

The samples were grown by molecular beam epitaxy (MBE) on planar Si (001) substrates and two-dimensional (2D) patterned ones with a period of 500 nm and pit depths and diameters of ~65 nm and 350 nm, respectively. Before loading into the MBE chamber, the Si substrates were dipped in a HF solution to create a hydrogen terminated surface. After 45 nm of Si buffer growth, 6.0, 9.0, and 12.0 monolayers (MLs) Ge were deposited at a substrate temperature of 720 °C and at a Ge growth rate of 0.03 Å/s. For comparison,

8 ML Ge were deposited on a planar Si substrate using the same growth conditions. Correspondingly, we obtained, for increasing Ge amounts, uniform arrays of pyramids, domes, and barns on patterned substrates, and randomly distributed islands on the planar substrates. The SiGe islands of different shapes were etched at room temperature in NHH solution [1:1 vol.(28% NH<sub>4</sub>OH):(31% H<sub>2</sub>O<sub>2</sub>)], which selectively etches Si<sub>1-x</sub>Ge<sub>x</sub> alloys over pure Si and shows an exponentially increasing etching rate with the Ge fraction  $x$ .<sup>12,14</sup> The surface morphology was recorded using AFM in tapping mode.

Figures 1(a)–1(d) show a sequence of 3D AFM images of the same surface area obtained after deposition of 12 ML Ge (barn-shaped islands) and after subsequent selective etching in NHH for 100, 280, and 500 min. We see that (i) for all the islands SiGe is etched symmetrically and (ii) the homogeneity of the shape and size of the residual island material is preserved after different etching times. (i) Indicates a sym-

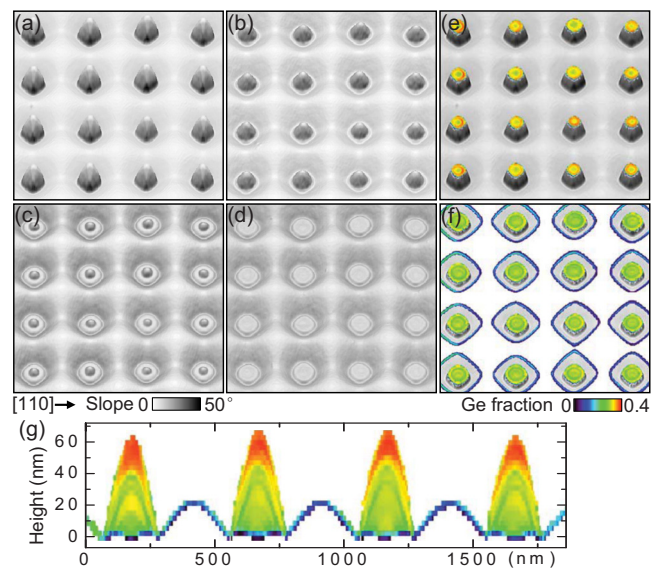


FIG. 1. (Color online) Sequence of 3D AFM images of the same surface area obtained after deposition of 12 ML Ge on patterned Si(001) with a period of 500 nm at 720 °C (a) and after selective etching in NHH solution for 100 (b), 280 (c), and 500 min (d). (e) and (f) Horizontal cross-sections of the islands shown in (a) with in-plane Ge compositions at heights of 36 nm and 10 nm with respect to the level of the island bases. (g) Vertical cross-cut of the Ge content across one island row shown in (a) passing through the island centers along the [110] direction.

<sup>a)</sup>Electronic mail: j.zhang@ifw-dresden.de.

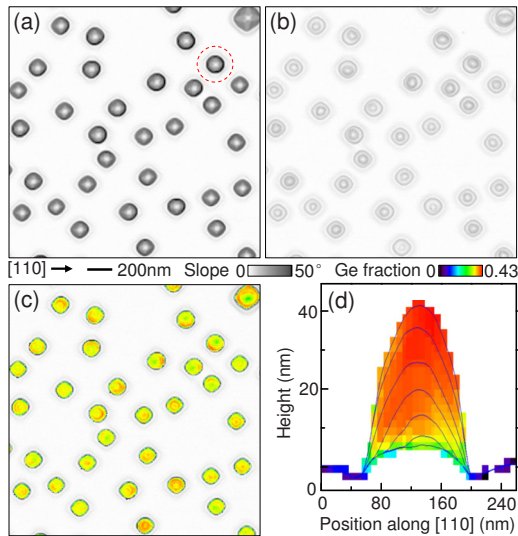


FIG. 2. (Color online) AFM images of a sample obtained after deposition of 8 ML Ge on planar Si(001) at 720 °C (a) and after selective etching in NHH solution for 55 min (b). The dashed circle in (a) marks a barn-shaped island. (c) Horizontal cross-cut of the islands shown in (a) with in-plane Ge composition at a height of 4 nm with respect to the level of the substrate. (d) Vertical cross-cut of the marked island shown in (a) with color-coded Ge distribution, passing through the island center along [110] direction.

metric Ge distribution for all islands and (ii) demonstrates that different islands in the array have similar composition distributions. Figures 1(e) and 1(f), respectively, show the horizontal cross-cuts parallel to the (001) plane of the Ge distribution for islands shown in Fig. 1(a) at heights of 36 and 10 nm, with respect to the level of the island bases. Figure 1(g) shows the vertical cross-sectional Ge composition on the (110) plane passing through the centers of one row of islands. A symmetric Ge distribution is clearly seen and all islands show similar Ge composition profiles within the uncertainties, which mainly originate from the registering of the AFM images after different etching steps.<sup>12</sup> (We note that, different from the results presented in Ref. 12, the island surface remains smooth after etching.)

In contrast, on planar substrates, islands obtained after the deposition of 8 ML Ge show a relatively broad size distribution with transition barns, barns and even dislocated superdomes, as shown in Fig. 2(a)—a superdome is seen on the top right corner of the image. Figure 2(b) displays the AFM image of these islands etched for 55 min in NHH and Fig. 2(c) shows their in-plane Ge composition at a height of 4 nm above the substrate level. For most of the coherent islands, slight lateral asymmetries in the composition associated with shape asymmetries are observed, similar to previous observations.<sup>12</sup> Interestingly, the island composition is asymmetric even for barns with an apparently symmetric shape [see the island marked by dashed circle in Fig. 2(a)]. Such an asymmetry is well noticeable in Fig. 2(d), which shows AFM linescans obtained at different etching stages and the derived cross-sectional Ge composition.

Islands grown on planar surfaces differ from islands grown on pit patterned substrates not only for their asymmetric composition profiles but also for the values of average Ge content  $x$  and volume:  $x$  is about 17% higher for barns on planar substrates ( $x \sim 35\%$ ) than on patterned substrates ( $x \sim 30\%$ ), in agreement with recent x-ray diffraction measurements showing a smaller Ge content for islands on pits;<sup>15</sup> the average island volume for islands on planar substrates ( $\sim 4$

$\times 10^5 \text{ nm}^3$ ) is about 2.5 times smaller than on patterned substrates ( $\sim 10^6 \text{ nm}^3$ ). We mainly ascribe these differences to a larger availability of Si flow on patterned substrates from the terraced pit sidewalls,<sup>16</sup> where the Si substrate is covered on average by a thinner Ge wetting layer.<sup>17</sup> The larger availability of Si leads to enhanced Si–Ge intermixing.

Since the island arrays remain homogeneous in shape, size and composition at all investigated stages of growth, we limit in the following the discussion to the compositional evolution of single islands. Figures 3(a)–3(i) show a sequence of 3D AFM images of individual islands prior to etching and after different etching times in NHH for a pyramid [(a)–(c)], a dome [(d)–(f)], and a barn [(g)–(i)], respectively. For all types of islands, the etching profiles are symmetric after different etching steps, indicating a symmetric Ge distribution. For the pyramid, the material at the edges is etched faster than at the corners [Fig. 3(b)], demonstrating that the corners are enriched with Si.<sup>18,19</sup> However, these features are not observed for the domes and barns, indicating a Ge redistribution during the evolution from pyramid to dome and barn. Figures 3(l)–3(n) show the in-plane Ge distributions for the different shapes at a height of 10 nm with respect to the level of the island bases,<sup>20</sup> while Figs. 4(a)–4(c) show AFM linescans at different stages of NHH etching and the derived cross-sectional Ge compositions. Both from the horizontal [Figs. 3(l)–3(n)] and vertical [Figs. 4(a)–4(c)] cross-cuts, we observe that at the bottom of the islands, e.g., at a height of 10 nm above the island base, the Ge fraction drops from  $\sim 35\%$  to 31% when a pyramid evolves into a dome, while no clear changes are observed when a dome transforms into a barn [see also Figs. 4(d) and 4(e)]. Furthermore, after the almost complete removal of the SiGe in the islands in NHH,<sup>14</sup> the bottom of the pit is  $\sim 9$  nm lower than the island base for the pyramid, while it is only  $\sim 5$  nm lower than the island base for the dome and is almost at the same level of the island base for the barn, as seen by comparing the bottommost linescans in Figs. 4(a)–4(c). These results indicate that the Ge content at the island base decreases as the island grows in size and is less than 10% for the barns after 12 ML Ge.

By assuming that shape transitions from pyramid to dome and from dome to barn are simply accomplished by progressive material accumulation at the island surface in a layer-by-layer fashion,<sup>4,5,21</sup> we would expect to find a pyra-

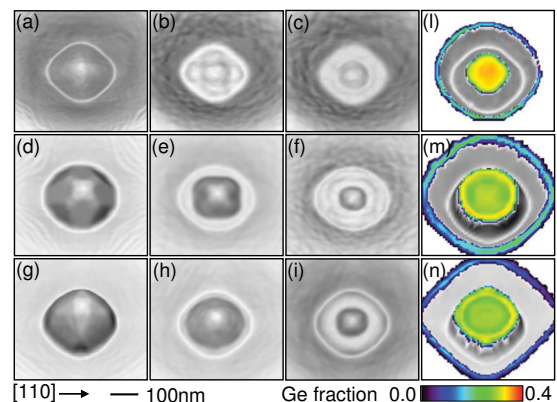


FIG. 3. (Color online) Sequences of 3D AFM images of individual islands prior to etching and after different etching times in NHH solution for pyramid [(a)–(c)], dome [(d)–(f)], and barn [(g)–(i)], respectively. [(l)–(m)] Horizontal cross-cuts of the pyramid, dome, and barn with in-plane compositions at a height of 10 nm with respect to the level of island bases.

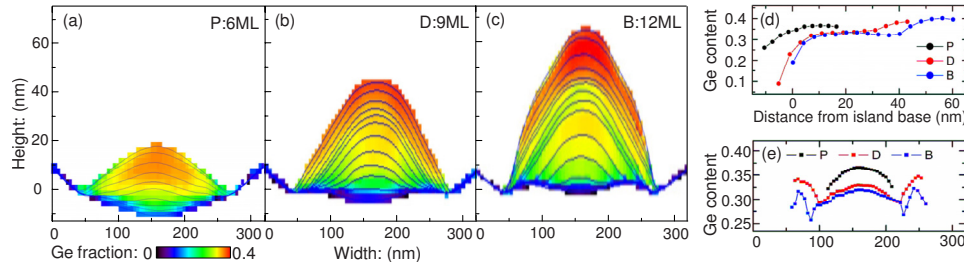


FIG. 4. (Color online) Cross-sectional Ge compositions on (110) planes passing through island centers for a pyramid (a), a dome (b), and a barn (c), grown on pit-patterned Si(001) at 720 °C. The level of the island bases is set as zero. [(d) and (e)] Ge compositions along the growth direction and the lateral [110] direction at a height of 10 nm with respect to the level of island bases, passing through the island centers for pyramid, dome, and barn, respectively.

mid (more precisely, the Ge distribution in the pyramid) “inside” the dome and a dome “inside” the barn.<sup>12</sup> However, the comparison of Figs. 4(a)–4(c) and of the linescans of Ge composition along the growth direction shown in Fig. 4(d) indicates that the data are not fully compatible with this picture. In fact, as noted above, the bottom region of the islands becomes Si-rich as pyramids transform into domes and barns. Furthermore the top and Ge-rich region ( $x \sim 38\%$ ) of the dome is replaced by a Ge-poorer region ( $x \sim 32\%$ ) in the barn, while the underlying Ge rich core is almost preserved. Finally the horizontal linescans for domes and barns shown in Fig. 4(e) indicate that there is a Si-rich shell (dip in the linescans) which appears to shift outwards when the domes transform into barns.

For islands grown on planar substrates, it has been previously shown that Si–Ge intermixing mainly occurs through surface diffusion and that islands change shape by accumulation of material at their surface.<sup>5,21</sup> However the results presented in Fig. 4 (for instance the Si enrichment of the island base) can be hardly explained by surface diffusion only. Although most of the Si incorporated into the islands must come from the surrounding substrate regions, the complex compositional evolution accompanying the island growth suggests that also “intraisland diffusion” occurs during Ge deposition.<sup>22</sup> This phenomenon was reported to take place, even at lower substrate temperatures, during annealing experiments in conditions inhibiting Si surface diffusion.<sup>22</sup> In our case we argue that the pits, by effectively pinning the island positions,<sup>23</sup> limit the efficient surface-mediated intermixing which is associated with island motion<sup>21</sup> and asymmetric composition profiles seen on planar surfaces (see Fig. 2). On the other hand, further experimental and theoretical work is needed to understand the mechanisms responsible for the fine but complex compositional gradients observed in SiGe islands grown on pit-patterned substrates.

In summary, we have investigated the Ge composition for islands both on patterned and planar substrates by AFM-based nanotomography. On patterned substrates the islands in an array have very similar composition distributions and each island shows a symmetric alloy distribution. Furthermore, the comparison of the Ge distributions in pyramids, domes and barns indicates that a redistribution of material involving not only surface processes occurs as the islands grow on pits.

We thank R. Gatti, F. Montalenti, L. Miglio, and F. Schäffler for helpful discussions and the EC d-DOTFET

(Grant No. 012150), the FWF (Grant No. SFB025), the GMe, Vienna, and the DFG (FOR 730) for support.

- <sup>1</sup>T. I. Kamins, E. C. Carr, R. S. Williams, and S. J. Rosner, *J. Appl. Phys.* **81**, 211 (1997).
- <sup>2</sup>G. Medeiros-Ribeiro, A. M. Bratkovski, T. I. Kamins, D. A. A. Ohlberg, and R. S. Williams, *Science* **279**, 353 (1998).
- <sup>3</sup>F. M. Ross, R. M. Tromp, and M. C. Reuter, *Science* **286**, 1931 (1999).
- <sup>4</sup>F. Montalenti, P. Raiteri, D. B. Migas, H. von Känel, A. Rastelli, C. Manzano, G. Costantini, U. Denker, O. G. Schmidt, K. Kern, and L. Miglio, *Phys. Rev. Lett.* **93**, 216102 (2004).
- <sup>5</sup>Y. Tu and J. Tersoff, *Phys. Rev. Lett.* **98**, 096103 (2007).
- <sup>6</sup>F. M. Ross, J. Tersoff, and R. M. Tromp, *Phys. Rev. Lett.* **80**, 984 (1998).
- <sup>7</sup>Z. Zhong and G. Bauer, *Appl. Phys. Lett.* **84**, 1922 (2004).
- <sup>8</sup>J. J. Zhang, M. Stoffel, A. Rastelli, O. G. Schmidt, V. Jovanović, L. K. Nanver, and G. Bauer, *Appl. Phys. Lett.* **91**, 173115 (2007).
- <sup>9</sup>C. Dais, G. Mussler, H. Sigg, E. Müller, H. H. Solak, and D. Grützmacher, *J. Appl. Phys.* **105**, 122405 (2009).
- <sup>10</sup>J. J. Zhang, F. Montalenti, A. Rastelli, N. Hrauda, D. Scopece, H. Groiss, J. Stangl, F. Pezzoli, F. Schäffler, O. G. Schmidt, L. Miglio, and G. Bauer, *Phys. Rev. Lett.* **105**, 166102 (2010).
- <sup>11</sup>M. Grydlik, M. Brehm, F. Hackl, H. Groiss, T. Fromherz, F. Schäffler, and G. Bauer, *New J. Phys.* **12**, 063002 (2010).
- <sup>12</sup>A. Rastelli, M. Stoffel, A. Malachias, T. Merdzhanova, G. Katsaros, K. Kern, T. H. Metzger, and O. G. Schmidt, *Nano Lett.* **8**, 1404 (2008).
- <sup>13</sup>A. Rastelli, M. Stoffel, U. Denker, T. Merdzhanova, and O. G. Schmidt, *Phys. Status Solidi A* **203**, 3506 (2006).
- <sup>14</sup>M. Stoffel, A. Malachias, T. Merdzhanova, F. Cavallo, G. Isella, D. Chrastina, H. von Känel, A. Rastelli, and O. G. Schmidt, *Semicond. Sci. Technol.* **23**, 085021 (2008).
- <sup>15</sup>T. U. Schüllli, G. Vastola, M.-I. Richard, A. Malachias, G. Renaud, F. Uhlík, F. Montalenti, G. Chen, L. Miglio, F. Schäffler, and G. Bauer, *Phys. Rev. Lett.* **102**, 025502 (2009).
- <sup>16</sup>G. Chen, H. Lichtenberger, G. Bauer, W. Jantsch, and F. Schäffler, *Phys. Rev. B* **74**, 035302 (2006).
- <sup>17</sup>J. J. Zhang, N. Hrauda, H. Groiss, A. Rastelli, J. Stangl, F. Schäffler, O. G. Schmidt, and G. Bauer, *Appl. Phys. Lett.* **96**, 193101 (2010).
- <sup>18</sup>U. Denker, M. Stoffel, and O. G. Schmidt, *Phys. Rev. Lett.* **90**, 196102 (2003).
- <sup>19</sup>G. Katsaros, G. Costantini, M. Stoffel, R. Esteban, A. M. Bittner, A. Rastelli, U. Denker, O. G. Schmidt, and K. Kern, *Phys. Rev. B* **72**, 195320 (2005).
- <sup>20</sup>For the vertical alignment, we assumed the bases of these islands at the same level. Our calculations of the amount of Si incorporated into the islands from the surroundings during the island evolution from pyramids to barns have proven that this assumption is reasonable.
- <sup>21</sup>U. Denker, A. Rastelli, M. Stoffel, J. Tersoff, G. Katsaros, G. Costantini, K. Kern, N. Y. Jin-Phillipp, D. E. Jesson, and O. G. Schmidt, *Phys. Rev. Lett.* **94**, 216103 (2005).
- <sup>22</sup>M. S. Leite, G. Medeiros-Ribeiro, T. I. Kamins, and R. S. Williams, *Phys. Rev. Lett.* **98**, 165901 (2007).
- <sup>23</sup>J. J. Zhang, A. Rastelli, H. Groiss, J. Tersoff, F. Schäffler, O. G. Schmidt, and G. Bauer, *Appl. Phys. Lett.* **95**, 183102 (2009).